

Computational Methods Used in the Study of Grafting 2-Chloroethyl Phosphonic Acid on Titania

SIMONA FUNAR-TIMOFEI, GHEORGHE ILIA

Institute of Chemistry

Romanian Academy

24 Mihai Viteazul Bvd., 300223-Timisoara

ROMANIA

timofei@acad-icht.tm.edu.ro, ilia@acadi-icht.tm.edu.ro

Abstract: - The surface of TiO₂ particles can be modified by phosphonic acids, this modification having several applications, like: photoelectrochemical cells based on nanocrystalline films of TiO₂, optical write-read-erase devices, enzymatic catalyses and plant growth regulator. Anchoring of organophosphorus derivatives on a titania surface is expected to involve both coordination of the phosphoryl oxygen to Lewis acid sites and condensation reactions between the surface hydroxyl groups Ti-OH and the P-OX and to lead to a strongly bind to the surface of transition metal oxides. This paper presents a theoretical study on grafting reactions of 2-chloroethyl phosphonic acid of titanium oxide surface. Starting from experimental X-ray data of the rutile crystal, several possible complexes with 2-chloroethyl phosphonic acid were built. The semiempirical PM6 quantum chemical approach was used in order to find out the way of anchoring the phosphonic moieties. The results thus obtained gave indications on the stability of the complex formation.

Key-Words: - computational methods, PM6, titania, 2-chloroethyl phosphonic acid, grafting, quantum chemistry

1 Introduction

Computational methods are widely applied in several fields, like: greenhouse modelling [1], power system optimization and control [2] and biochemical processes [3], and, also, in the chemistry of solid state.

During the past decade, interest in chemical reactions occurring at metal oxide-aqueous solution interfaces has increased significantly because of their importance in a variety of fields, including atmospheric chemistry, heterogeneous catalysis and photocatalysis, chemical sensing, corrosion science, environmental chemistry and geochemistry, metallurgy and ore beneficiation, metal oxide crystal growth, soil science, semiconductor manufacturing and cleaning, and tribology [4]. Oxide surface reactivity is exploited in many industrial processes involving catalysis and photolysis and is fundamental to environmental chemistry and geochemistry. Indeed, hydrous oxides of Al, Fe, Mn, and aluminosilicates such as clays are ubiquitous in the natural environment, and their surface chemical properties control such important phenomena as nutrient and contaminant element release and uptake, pH buffering, water quality, and soil rheological properties. These surfaces function as templates for the growth of other solid phases and

as a matrix for microflora. Given the importance of metal oxide surfaces in these processes, surprisingly little is known about their atomic-scale structure and chemical reactivity, particularly in aqueous environments. Chemical interactions at metal oxide-aqueous solution interfaces are extremely complex, and it is safe to say that understanding such interactions on a fundamental atomic level has not been achieved.

As metal-carbon bonds are generally not sufficiently stable toward hydrolysis, anchoring an organic group to a metal oxide support requires the use of coupling molecules. Organophosphorus compounds offer a promising alternative in the coupling of organic components to metal oxides other than silica; thus, being reported a novel sol-gel route to metal oxide/phosphonate covalent hybrid solids [5]. The surface modification of an inorganic support with organophosphorus coupling agents is an important way to hybrid materials [6]. This route has been applied to a variety of supports, including metal oxides, metals, aluminosilicates, silica, metal hydroxides, and carbonates.

The modification of alumina surfaces with phosphonic acids RPO(OH)₂ is currently attracting growing interest in fields such as self-assembled monolayers [7], and ceramic membranes [8].

However the balance between surface complexation (namely grafting) and surface phase transformation (namely deposition of bulk metal phosphonate phases) [9] depends on the experimental conditions. Surface complexation involves both the coordination of the phosphoryl oxygens to Lewis acid sites, and the condensation of P-OH groups of the phosphonic acid with the surface hydroxyl groups Al-OH [10]. Alumina provides excellent properties as a support. These include ease of diffusion of reactant in the pore structure and a large available specific surface, leading to its high popularity as a support for both heterogeneous catalysis and chromatography. Phosphonyl groups are known to form very stable networks in aluminium phosphate and in ALPOs [11]. Studies on Ti-Al binary alloy and Ti-Al-Nb ternary alloy have been reported [12].

Also the surface of TiO₂ particles can be modified by phosphonic acids, this modification having several applications, like: photo-electrochemical cells based on nanocrystalline films of TiO₂, optical write-read-erase devices, enzymatic catalyses and plant growth regulator [13].

Mutin et al consider that the anchoring of organophosphorus derivatives on a titania surface is expected to involve both coordination of the phosphoryl oxygen to Lewis acid sites and condensation reactions between the surface hydroxyl groups Ti-OH and the P-OX (X = H, Me₃Si, Et) groups [14].

The bonding mode of organophosphorous coupling agent surface species appears to depend strongly on the nature of both organophosphorous coupling agent and the surface, and on the conditions of the surface modification [6]. In the case of phosphonic and phosphinic acids it was shown that, depending on the oxide chemical stability and on the grafting conditions (temperature pH, concentration of organophosphorous coupling agent), a dissolution-precipitation mechanism can be operative, leading to the formation of a metal phosphonate or phosphinate phase, even in case of chemically stable TiO₂. This mechanism implies the cleavage of the Ti-O-Ti bridges by the organophosphorus acid; considering the excellent chemical stability of TiO₂, assistance to the cleavage by coordination of phosphoryl group was proposed.

In a previous study [15] the grafting reaction of vinyl phosphonic acid on titanium oxide was modelled by PM6 [16]. The monodentate hybrid was found as most stable of all the studied hybrids. Stewart indicates that the length which involves oxygen forming a dative bond to titanium obtained by PM6 in coordination complexes is typically too

long, by 0.1 to 0.3 Å, but the PM6 approach has a better accuracy in predicting heats of formation for compounds of interest in biochemistry in comparison to Hartree Fock or B3LYP DFT methods, using the 6-31G(d) basis set [16].

In this paper the stability of titania grafted with 2-chloroethyl phosphonic acid was studied using computational methods. Several possible hybrids were considered and energy minimized by PM6 in vacuum in the range of temperatures from 298 until 400 K. The reaction enthalpies were calculated from the formation enthalpies thus obtained. The results gave indications on the influence of temperature and on the stability of the complex formation.

2 Hybrid construction

The bulk rutile structure is given by 6-fold coordinated Ti^{VI} atoms and 3-fold coordinated O atoms [17]. Two of the O-Ti bonds are 1.946 Å long; the third one is longer, 1.984 Å. The nonhydroxylated (110) surface stems from the relaxation of the rutile bulk structure cleaved by the (110) plane. Only rows of bridging oxygens (each bonded to two underlying Ti atoms) protrude out of the layer containing surface titanium and oxygen atoms. In between these rows there are rows of 3-fold coordinated O and 5-fold coordinated terminal Ti^V atoms in the same surface plane.

Because the problems of interpretation exist, the surface structures are obvious for layered minerals but are very questionable for other minerals [18]. In some cases, crystallographic data and common sense allow deduction of the different variants of atomic arrangement on the surface. In addition, the modeling of surface structure is not the only problem.

The difficulties of the structural analysis adduced above are related primarily to the subionic structures, which consist of atoms with coordination numbers exceeding their valences. These are structures of the most common oxides and hydroxides of Fe, Al, Ti, Mn, and other minerals having close-packed arrangements of oxygen atoms.

A hydrated titanium oxide crystal was built by Hyperchem package [19], taking into account the most stable 110 plane of the unit cell of the titanium oxide crystal [20] (see figure 1).

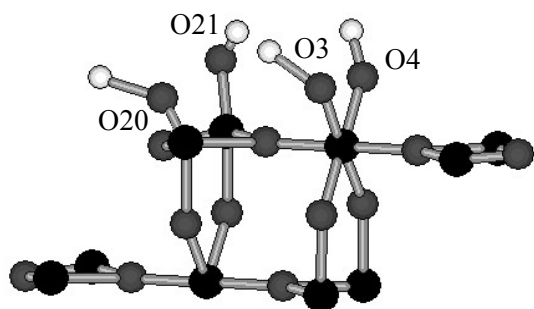


Fig. 1 Structure of crystal fragment of hydrated titanium oxide

○ - hydrogen atom; ● - oxygen atom;
● - titanium atom

The structure of 2-chlorethyl phosphonic acid was built by the Winmostar program [21] and energy minimized by the PM6 method [16]. SCF convergence of 10^{-10} , keyword PRECISE and a gradient of 10^{-2} were used. The optimized structure thus obtained (see figure 2) was further used in hybrid construction.

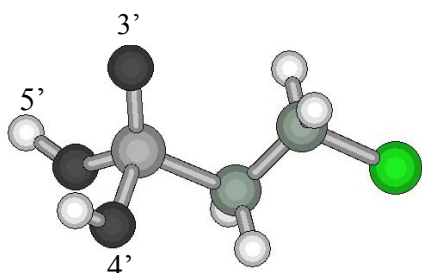
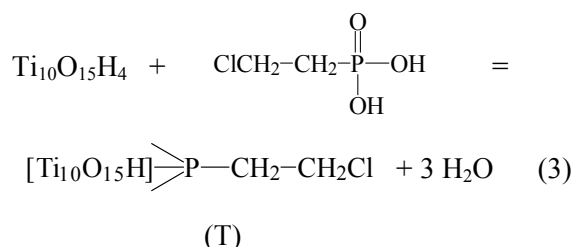
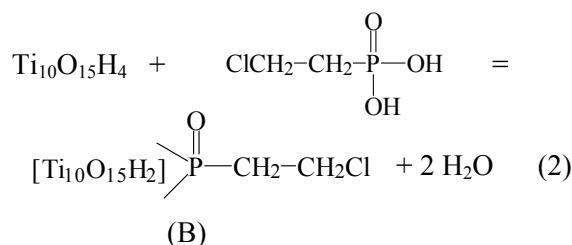
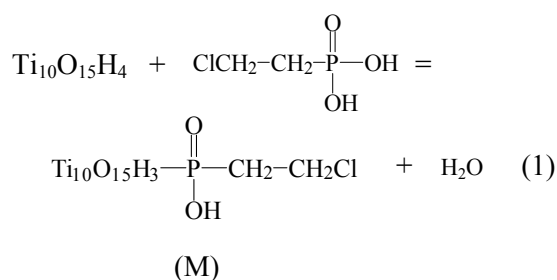


Fig. 2 Optimized structure of the 2-chlorethyl phosphonic acid

○ - hydrogen atom; ● - oxygen atom;
● - phosphorus atom; ● - carbon atom;
● - chlorine atom;

Startig from the optimized structure of the 2-chlorethyl phosphonic acid and from the hydrated titanium oxide fragment, hybrids of grafted mono-, bi- and tridentate phosphonic units on titania surface were built by the Winmostar [21] and Vega ZZ v. 2.0.8.60 [22] programs.

Following reactions of hybrid formation were considered:



where M represents the monodentate hybrid, B – the bidentate hybrid, T – the tridentate hybrid. In addition, hybrids formed by coordinative bonds between the phosphoryl oxygen atoms and titanium atoms were considered too. Hybrids M_{12} , M_{13} and M_{14} (see table 1) were similar to the hybrids M_9 , M_{10} and M_{11} , except the position of the 2-chlorethyl phosphonic acid, which was rotated to a mirror image position.

The Boltzmann distribution predicts the distribution function for the fractional number of particles N_i/N occupying a set of states i which each has energy E_i [23, 24]:

$$\frac{N_i}{N} = \frac{g_i e^{-E_i/k_B T}}{Z(T)} \quad (4)$$

where k_B is the Boltzmann constant, T is temperature (assumed to be a sharply well-defined quantity), g_i is the degeneracy, or number of states having energy E_i , N is the total number of particles and N_i the molecules having the energy E_i :

$$N = \sum_i N_i \quad (5)$$

and $Z(T)$ is called the partition function, which can be seen to be equal to

$$Z(T) = \sum_i g_i e^{E_i/k_B T} \quad (6)$$

The Boltzmann distribution is often expressed in terms of $\beta = 1/k_B T$ where β is referred to as thermodynamic beta. The term $\exp(-\beta E_i)$ or $\exp(-E_i/k_B T)$, which gives the (unnormalised) relative probability of a state, is called the Boltzmann factor. The Boltzmann constant can be replaced by the gas universal constant (R), if the energies from the Boltzmann distribution are replaced by molar energies.

For a distribution of n low energy hybrids in a given sample, the fraction f_i of a specific hybrid was expressed by the Boltzmann distribution, according to the following equation:

$$f_i = \frac{e^{-\frac{E_i}{RT}}}{\sum_{j=1}^n e^{-\frac{E_j}{RT}}} \quad (7)$$

where E_i represents the formation enthalpy of the i^{th} hybrid

T – the temperature

R – the universal gas constant

E_j – the total energy (which is proportional to the formation enthalpy) of the j^{th} hybrid

n – number of hybrids

The Boltzmann factor f_i is a weight function related to the percentage contribution of a given conformation to the conformational population of the compound.

3 Results and Discussion

The hybrid structures were energy minimized in vacuum by the PM6 semiempirical method included in the MOPAC 2007 program [16].

The keyword PRECISE and a gradient of 10^{-1} were used. From these calculations the enthalpies of formation at 298 K were obtained. The vacuum reaction enthalpy of each hybrid at 298 K was then calculated. The structures of minimum energy thus obtained were further used for the calculation of the reaction heat at different temperatures.

From the reaction enthalpies of each hybrid calculated at 298 K (see table 1) hybrid M_9 (similarly with M_{13}) had the highest negative value of the reaction enthalpy-with respect to the monodentate

hybrids, hybrid B_{14} (similarly with B_{15}) -with respect to the bidentate hybrids and T_{18} (the same with T_{22})-with respect to the tridentate hybrids. From the inspection of reaction enthalpies of all hybrids it was concluded that the monodentate hybrid was the most stable and probable to be formed by grafting reaction.

Figures 3-8 present the minimized hybrid structures.

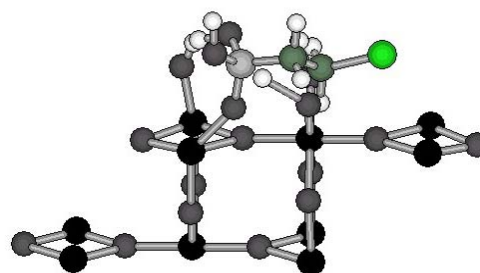


Fig. 3 Structure of monodentate hybrid M_9 before energy minimization

○ - hydrogen atom; ● - oxygen atom;
 ● - phosphorus atom; ● - carbon atom;
 ● - chlorine atom; ● - titanium atom

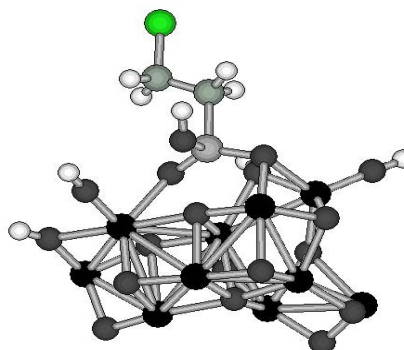


Fig. 4 Energy minimized structure of monodentate hybrid M_9

○ - hydrogen atom; ● - oxygen atom;
 ● - phosphorus atom; ● - carbon atom;
 ● - chlorine atom; ● - titanium atom

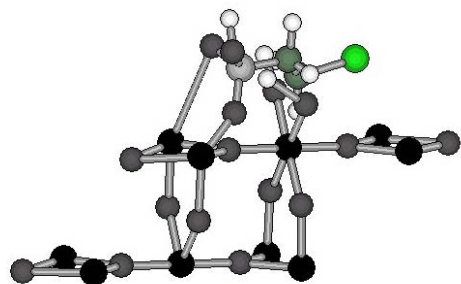


Fig. 5 Structure of bidentate hybrid B₁₄ before energy minimization

○ - hydrogen atom; ● - oxygen atom;
 ● - phosphorus atom; ● - carbon atom;
 ● - chlorine atom; ● - titanium atom

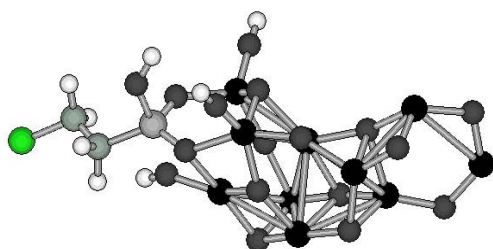


Fig. 6 Energy minimized structure of bidentate hybrid B₁₄

○ - hydrogen atom; ● - oxygen atom;
 ● - phosphorus atom; ● - carbon atom;
 ● - chlorine atom; ● - titanium atom

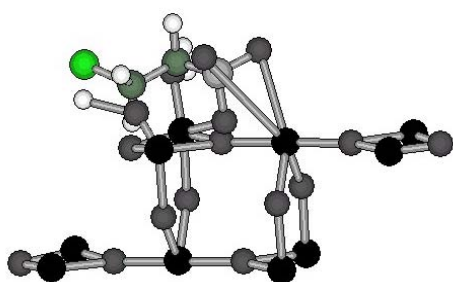


Fig. 7 Energy minimized structure of tridentate hybrid T₁₈ before energy minimization

○ - hydrogen atom; ● - oxygen atom;
 ● - phosphorus atom; ● - carbon atom;
 ● - chlorine atom; ● - titanium atom

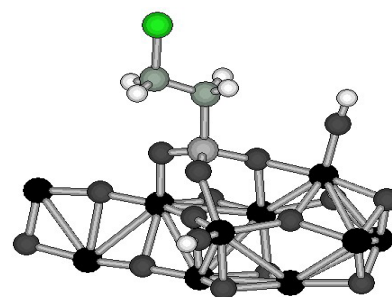


Fig. 8 Energy minimized structure of tridentate hybrid T₁₈

○ - hydrogen atom; ● - oxygen atom;
 ● - phosphorus atom; ● - carbon atom;
 ● - chlorine atom; ● - titanium atom

Taking into account the enthalpy of formation at 298 K the hybrid f_1 fraction, with respect to the number of hybrids of each type, was calculated with respect to each type of hybrid. The f_1 values (see table 2) confirmed that the mostly stable hybrids were the M₉, B₁₄ and T₁₈ hybrids, respectively.

The f_2 fraction with respect to the number of hybrids of all types was calculated, neglecting the difference of one, respectively two hydrogen atoms between the different types of hybrids. The f_2 values (see table 2) indicate as most stable the M₉ monodentate hybrid, in accordance to the biggest negative value of the reaction enthalpy and the less stable the tridentate T₁₈ hybrid.

Table 1. Hybrid structures (M = monodentate, B = bidentate, T = tridentate), enthalpy of formation at 298 k (ΔH_f), reaction enthalpy at 298 k (ΔH_r)

No.	Hybrid name*	ΔH_f kcal/mol	ΔH_r kcal/mol
1	M ₁ (O20*-O4'**)	-1814.6	-132.6
2	M ₂ (O21*-O4'**)	-1733.4	-51.3
3	M ₃ (O4*-O4'**)	-1667.5	14.5
4	M ₄ (O3*-O4'**)	-1739.9	-57.8
5	M ₅ (O20*-O5'**)	-1743.2	-61.2
6	M ₆ (O4*-O5'**)	-1718.7	-36.6
7	M ₇ (O3*-O5'**)	-1814.4	-132.3
8	M ₈ (O21*-O5'**)	-1658.5	23.5
9	M ₉ (O20*-O3'**)	-1864.2	-182.1
10	M ₁₀ (O21*-O3'**)	-1791.9	-109.9
11	M ₁₁ (O3*-O3'**)	-1838.	-156.0
12	M ₁₂ (O21*-O3'**)	-1772.8	-90.7
13	M ₁₃ (O20*-O3'**)	-1864.2	-182.1
14	M ₁₄ (O3*-O3'**)	-1772.8	-90.7
15	B ₁ (O4'*-O20**, O5'*-O21**)	-1714.4	-86.6
16	B ₂ (O4'*-O20**, O5'*-O3'')	-1650.1	-22.3

17	B ₃ (O4'*-O20**, O5'*-O4**)	-1691.2	-63.4
18	B ₄ (O4'*-O14**, O5'*-O20**)	-1691.2	-63.4
19	B ₅ (O4'*-O4**, O5'*-O21**)	-1695.7	-67.9
20	B ₆ (O4'*-O4**, O5'*-O3**)	-1681.8	-54.0
21	B ₇ (O4'*-O21**, O5'*-O20**)	-1755.8	-128.0
22	B ₈ (O4'*-O21**, O5'*-O4**)	-1444.4	183.2
23	B ₉ (O4'*O21**, O5'*-O3**)	-1452.8	174.8
24	B ₁₀ (O4'*-O3**, O5'*-O21**)	-1452.8	174.8
25	B ₁₁ (O4'*-O3**, O5'*-O20**)	-1621.	6.6
26	B ₁₂ (O4'*-O3**, O5'*-O4**)	-1701.1	-73.3
27	B ₁₃ (O5'*-O20**, O3'*-O21**)	-1615.9	11.7
28	B ₁₄ (O4'*-O21**, O3'*-O20**)	-1785.9	-158.2
29	B ₁₅ (O4'*-O21**, O3'*-O4**)	-1785.9	-158.2
30	B ₁₆ (O5'*-O20**, O3'*-O4**)	-1615.9	11.7
31	B ₁₇ (O4'*-O20**, O3'*-O21**)	-1710.4	-82.6
32	B ₁₈ (O4'*-O20**, O3'*-O4**)	-1710.4	-82.6
33	B ₁₉ (O5'*-O21**, O3'*-O20**)	-1675.5	-47.8
34	B ₂₀ (O5'*-O21**, O3'*-O4**)	-1675.5	-47.8
35	T ₁ (O4'*-O20**, O5'*-O21**, O3'*-O4**)	-1581.4	-7.9
36	T ₂ (O4'*-O20**, O5'*-O4**, O3'*-O3**)	-1706.9	-133.4
37	T ₃ (O4'*-O4**, O5'*-O21**, O3'*-O20**)	-1662.8	-89.3
38	T ₄ (O4'*-O4**, O5'*-O21**, O3'*-O3**)	-1662.8	-89.3
39	T ₅ (O4'*-O3**, O5'*-O21**, O3'*-O20**)	-1679.5	-106.1
40	T ₆ (O4'*-O3**, O5'*-O21**, O3'*-O4**)	-1679.5	-106.1

41	T ₇ (O4'*-O21**, O5'*-O20**, O3'*-O4**)	-1717.1	-143.6
42	T ₈ (O4'*-O4**, O5'*-O20**, O3'*-O21**)	-1661.3	-87.9
43	T ₉ (O4'*-O21**, O3'*-O20**, O5'*-O3**)	-1717.2	-143.7
44	T ₁₀ (O4'*-O4**, O5'*-O20**, O3'*-O3**)	-1661.3	-87.9
45	T ₁₁ (O4'*-O3**, O5'*-O20**, O3'*-O21**)	-1690.2	-116.7
46	T ₁₂ (O4'*-O3**, O5'*-O20**, O3'*-O4**)	-1690.2	-116.7
47	T ₁₃ (O4'*-O21**, O5'*-O4**, O3'*-O20**)	-1694.8	-121.3
48	T ₁₄ (O4'*-O21**, O5'*-O4**, O3'*-O3**)	-1694.8	-121.3
49	T ₁₅ (O4'*-O21**, O5'*-O3**, O3'*-O20**)	-1717.2	-143.7
50	T ₁₆ (O4'*-O20**, O5'*-O4**, O3'*-O21**)	-1607.8	-34.4
51	T ₁₇ (O4'*-O20**, O5'*-O3**, O3'*-O21**)	-1643.8	-70.4
52	T ₁₈ (O4'*-O4**, O5'*-O3**, O3'*-O21**)	-1730.2	-156.7
53	T ₁₉ (O4'*-O3**, O5'*-O4**, O3'*-O20**)	-1484.1	89.3
54	T ₂₀ (O4'*-O3**, O3'*-O21**, O5'*-O4**)	-1484.1	89.3
55	T ₂₁ (O4'*-O20**, O5'*-O3**, O3'*-O4**)	-1643.8	-70.4
56	T ₂₂ (O4'*-O4**, O5'*-O3**, O3'*-O20**)	-1730.2	-156.7

* positions of oxygen atoms of hydrated titanium oxide (see figure 1) involved in the hybrid construction

** positions of oxygen atoms of 2-chlorethyl phosphonic acid (see figure 2) involved in the hybrid construction

Table 2. Hybrid structures (M = monodentate, B = bidentate, T = tridentate) formed by grafting 2-chloroethyl phosphonic acid on titanium oxide, hybrid fraction with respect to each type of hybrid (f_1), hybrid fraction with respect to all types of hybrids (f_2)

No.	Hybrid name	f_1	f_2
1	M ₁	3.17×10^{-37}	3.17×10^{-37}
2	M ₂	1.27×10^{-96}	1.27×10^{-96}
3	M ₃	8.3×10^{-145}	8.35×10^{-145}
4	M ₄	7.3×10^{-92}	7.30×10^{-92}
5	M ₅	1.92×10^{-89}	1.92×10^{-89}
6	M ₆	2.3×10^{-107}	2.31×10^{-107}
7	M ₇	2.12×10^{-37}	2.12×10^{-37}
8	M ₈	2.2×10^{-151}	2.23×10^{-151}
9	M ₉	0.50	5.00×10^{-01}
10	M ₁₀	8.02×10^{-54}	8.02×10^{-54}
11	M ₁₁	4×10^{-20}	4.00×10^{-20}
12	M ₁₂	8.13×10^{-68}	8.13×10^{-68}
13	M ₁₃	0.500414	5.00×10^{-01}
14	M ₁₄	8.13×10^{-68}	8.13×10^{-68}
15	B ₁	2.52×10^{-53}	8.04×10^{-71}
16	B ₂	2.3×10^{-100}	7.31×10^{-118}
17	B ₃	2.7×10^{-70}	8.62×10^{-88}
18	B ₄	2.7×10^{-70}	8.62×10^{-88}
19	B ₅	5.18×10^{-67}	1.65×10^{-84}
20	B ₆	3.5×10^{-77}	1.12×10^{-94}
21	B ₇	4.52×10^{-23}	1.44×10^{-40}
22	B ₈	1.1×10^{-250}	3.43×10^{-268}
23	B ₉	1.5×10^{-244}	4.75×10^{-262}
24	B ₁₀	1.5×10^{-244}	4.75×10^{-262}
25	B ₁₁	1.4×10^{-121}	4.58×10^{-139}
26	B ₁₂	4.83×10^{-63}	1.54×10^{-80}
27	B ₁₃	2.6×10^{-125}	8.41×10^{-143}
28	B ₁₄	0.50	1.60×10^{-18}
29	B ₁₅	0.50	1.60×10^{-18}
30	B ₁₆	2.6×10^{-125}	8.41×10^{-143}
31	B ₁₇	2.94×10^{-56}	9.40×10^{-74}
32	B ₁₈	2.94×10^{-56}	9.40×10^{-74}
33	B ₁₉	1.01×10^{-81}	3.22×10^{-99}
34	B ₂₀	1.01×10^{-81}	3.22×10^{-99}
35	T ₁	7.8×10^{-110}	2.28×10^{-128}
36	T ₂	4.53×10^{-18}	1.33×10^{-36}
37	T ₃	2.59×10^{-50}	7.57×10^{-69}
38	T ₄	2.59×10^{-50}	7.57×10^{-69}
39	T ₅	4.65×10^{-38}	1.36×10^{-56}
40	T ₆	4.65×10^{-38}	1.36×10^{-56}
41	T ₇	1.3×10^{-10}	3.80×10^{-29}
42	T ₈	2.25×10^{-51}	6.59×10^{-70}
43	T ₉	1.56×10^{-10}	4.57×10^{-29}
44	T ₁₀	2.25×10^{-51}	6.59×10^{-70}

45	T ₁₁	2.79×10^{-30}	8.17×10^{-49}
46	T ₁₂	2.79×10^{-30}	8.17×10^{-49}
47	T ₁₃	6.34×10^{-27}	1.85×10^{-45}
48	T ₁₄	6.34×10^{-27}	1.85×10^{-45}
49	T ₁₅	1.56×10^{-10}	4.57×10^{-29}
50	T ₁₆	1.73×10^{-90}	5.05×10^{-109}
51	T ₁₇	3.56×10^{-64}	1.04×10^{-82}
52	T ₁₈	0.50	1.46×10^{-19}
53	T ₁₉	5.8×10^{-181}	1.71×10^{-199}
54	T ₂₀	5.8×10^{-181}	1.71×10^{-199}
55	T ₂₁	3.56×10^{-64}	1.04×10^{-82}
56	T ₂₂	0.50	1.46×10^{-19}

The heats of reaction of the minimum energy structures thus obtained were calculated at different temperatures, in the range from 298 until 400 K, by the MOPAC 2007 program [16]. Table 3 presents the thermodynamic properties of the most stable M₉ monodentate hybrid. Low temperatures favor the hybrid formation, similarly to [15].

Table 3. Thermodynamic properties of the M₉ monodentate hybrid and reaction enthalpy at the T temperature ($(\Delta H_f)_T$)

T (K)	Thermodynamic properties*	$(\Delta H_f)_T$ (kcal/mol)
298	ΔH_f (kcal/mol)	-183.92
	H (cal/mol)	
	c_p (cal/K/mol)	
	S (cal/K/mol)	
300	ΔH_f (kcal/mol)	-183.92
	H (cal/mol)	
	c_p (cal/K/mol)	
	S (cal/K/mol)	
305	ΔH_f (kcal/mol)	-183.91
	H (cal/mol)	
	c_p (cal/K/mol)	
	S (cal/K/mol)	
310	ΔH_f (kcal/mol)	-183.91
	H (cal/mol)	
	c_p (cal/K/mol)	
	S (cal/K/mol)	
315	ΔH_f (kcal/mol)	-183.9
	H (cal/mol)	
	c_p (cal/K/mol)	
	S (cal/K/mol)	
320	ΔH_f (kcal/mol)	-183.91
	H (cal/mol)	
	c_p (cal/K/mol)	
	S (cal/K/mol)	

325	ΔH_f (kcal/mol)	-183.91
	H (cal/mol)	
	c_p (cal/K/mol)	
	S (cal/K/mol)	
330	ΔH_f (kcal/mol)	-183.91
	H (cal/mol)	
	c_p (cal/K/mol)	
	S (cal/K/mol)	
335	ΔH_f (kcal/mol)	-183.91
	H (cal/mol)	
	c_p (cal/K/mol)	
	S (cal/K/mol)	
340	ΔH_f (kcal/mol)	-183.9
	H (cal/mol)	
	c_p (cal/K/mol)	
	S (cal/K/mol)	
345	ΔH_f (kcal/mol)	-183.9
	H (cal/mol)	
	c_p (cal/K/mol)	
	S (cal/K/mol)	
350	ΔH_f (kcal/mol)	-183.89
	H (cal/mol)	
	c_p (cal/K/mol)	
	S (cal/K/mol)	
355	ΔH_f (kcal/mol)	-183.89
	H (cal/mol)	
	c_p (cal/K/mol)	
	S (cal/K/mol)	
360	ΔH_f (kcal/mol)	-183.901
	H (cal/mol)	
	c_p (cal/K/mol)	
	S (cal/K/mol)	
365	ΔH_f (kcal/mol)	-183.89
	H (cal/mol)	
	c_p (cal/K/mol)	
	S (cal/K/mol)	
370	ΔH_f (kcal/mol)	-183.89
	H (cal/mol)	
	c_p (cal/K/mol)	
	S (cal/K/mol)	
375	ΔH_f (kcal/mol)	-183.59
	H (cal/mol)	
	c_p (cal/K/mol)	
	S (cal/K/mol)	
380	ΔH_f (kcal/mol)	-183.89
	H (cal/mol)	
	c_p (cal/K/mol)	
	S (cal/K/mol)	

385	ΔH_f (kcal/mol)	-183.88
	H (cal/mol)	
	c_p (cal/K/mol)	
	S (cal/K/mol)	
390	ΔH_f (kcal/mol)	-183.89
	H (cal/mol)	
	c_p (cal/K/mol)	
	S (cal/K/mol)	
395	ΔH_f (kcal/mol)	-183.88
	H (cal/mol)	
	c_p (cal/K/mol)	
	S (cal/K/mol)	
400	ΔH_f (kcal/mol)	-183.895
	H (cal/mol)	
	c_p (cal/K/mol)	
	S (cal/K/mol)	

* ΔH_f – standard enthalpy of formation,
H – enthalpy, c_p – caloric capacity, S – entropy,
T - temperature

The negative values of the heat of formation at 298 K of most hybrids point out the possibility of formation of all the three types of considered hybrids, with highest probability of monodentate hybrid formation and the lower probability of tridentate hybrid formation.

Structural descriptors, like: the solvent accessible surface and volume and the van der Waals surface and volume [25] of energy minimized hybrids have been calculated by the Winmostar program [22]. For the M_9 hybrid following structural parameters were obtained: the van der Waals surface of 435.479 \AA^2 , the van der Waals volume of $403,836 \text{ \AA}^3$, the solvent accessible surface of 622.330 \AA^2 , the solvent accessible volume of 1127.700 \AA^3 (calculated for water used as solvent, with the water radius of 1.4 \AA).

3 Conclusion

Hybrid formation by the 2-chloethyl phosphonic acid grafting on titanium oxide was simulated by the semiempirical PM6 method. Starting from a fragment of titanium oxide structure (built from experimental X-ray data) three types of hybrids: monodentate, bidentate and tridentate were considered. The hybrids were energy minimized by the semiempirical PM6 method in vacuum at 298 K. The reaction enthalpies at 298 K were calculated from the formation enthalpies thus obtained. These values indicated the highest probability of M_9 monodentate hybrid formation. Reaction enthalpies

in the range of temperatures from 298 K to 400 K for the most stable hybrid were further calculated. It was observed that lower temperatures favor the monodentate hybrid formation

Acknowledgement

The authors thank Prof. Mircea Mracec from the Institute of Chemistry of Timisoara (Romania), for giving access to the to the Hyperchem program and for useful discussions and to Prof. James J. P. Stewart (Stewart Computational Chemistry, web: <http://OpenMOPAC.net>) for kindly giving the permission to work with the MOPAC 2007 program.

References:

- [1] N. Pessel, J. -F. Balmat, Principal Component Analysis for Greenhouse Modelling, *WSEAS TRANSACTIONS on SYSTEMS*, Vol. 7, No. 9, 2008, pp. 24-30.
- [2] R.C. Berredo, L.N. Canha, P.Ya. Ekel, L.C.A. Ferreira and M.V.C. Maciel, Experimental Design and Models of Power System, Optimization and Control, *WSEAS TRANSACTIONS on SYSTEMS and CONTROL*, Vol. 3, No. 1, 2008, pp. 40-49.
- [3] V. Galvanauskas, R. Simutis, Software tool for efficient hybrid model-based design of biochemical processes, *WSEAS TRANSACTIONS on BIOLOGY and BIOMEDICINE*, Vo. 4, No. 9, 2007, pp. 136-144.
- [4] G. E. Brown, Jr, V. E. Henrich, W. H. Casey, D. L. Clark, C. Eggleston, D. W. Goodman, M. Grätzel, G. Maciel, M. I. McCarthy, K. H. Nealson, D. A. Sverjensky, M. F. Toney, J. M. Zachara, Metal Oxide Surfaces and Their Interactions with Aqueous Solutions and Microbial Organisms *Chem. Rev.*, Vol. 99, 1999, pp. 77-174.
- [5] G. Guerrero, P. H. Mutin, A. Vioux, Mixed Nonhydrolytic/Hydrolytic Sol-Gel Routes to Novel Metal Oxide/Phosphonate Hybrids, *Chem. Mater.* Vol. 12, 2000, pp.1268-1272.
- [6] A. Vioux, J. Le Bideau, P. H. Mutin, D. Leclercq, Hybrid Organic-Inorganic Materials Based on Organophosphorus Derivatives, *Top. Curr. Chem.* Vol. 232, 2004, pp. 145- 174.
- [7] W. Gao, L. Dickinson, C. Grozinger, F. G. Morin, L. Reven, Self-Assembled Monolayers of Alkylphosphonic Acids on Metal Oxides, *Langmuir* Vol. 12, 1996, pp. 6429-6435.
- [8] J. Caro, M. Noack, P. Kolsch, Chemically modified ceramic membranes, *Microporous Mesoporous Mater.* Vol. 22, 1998, pp. 321-332.
- [9] E. Laiti, P. Persson, L. O. Ohman, Balance between Surface Complexation and Surface Phase Transformation at the Alumina/Water Interface, *Langmuir* Vol. 14, 1998, pp. 825-831.
- [10] G. Guerrero, G. Chaplais, P. H. Mutin, J. Le Bideau, D. Leclercq, A. Vioux, Grafting of Alumina by Diphenylphosphinate Coupling Agents, *Mat. Res. Soc. Symp. Proc.* Vol. 628, 2000, pp. CC6.6.1-CC6.6.6.
- [11] D. Villemin, B. Moreau, F. Siméon, G. Maheut, C.Fernandez, V. Montouillout, V. Caignaert, P.-A. Jaffrès, A one step process for grafting organic pendants on alumina *via* the reaction of alumina and phosphonate under microwave irradiation, *Chem. Commun.*, 2001, pp. 2060–2061.
- [12] S. Nansaarnng, P. Srichands, Synthesis of intermetallic compounds of Ti-Al and Ti-Al-Nb systems and their properties, *Proceedings of the 4th WSEAS Int. Conf. on HEAT TRANSFER, THERMAL ENGINEERING and ENVIRONMENT*, Elounda, Greece, August 21-23, 2006, pp. 254-257.
- [13] G. Guerrero, P.H. Mutin, A. Vioux, Anchoring of Phosphonate and Phosphinate Coupling Molecules on Titania Particles, *Chem. Mater.* Vol. 13, 2001, pp. 4367- 4373.
- [14] P.H. Mutin, G. Guerrero, A. Vioux, Hybrid materials from organophosphorus coupling molecules, *J. Mater. Chem.* Vol. 15, 2005, pp. 3761- 3768.
- [15] S. Funar-Timofei, G. Ilia, Theoretical study of organic-inorganic hybrids obtained by grafting reaction of vinyl phosphonic acid on titanium oxide, *J. Optoelectron. Adv. Mat.*, Vol. 9, 2007, pp. 3933-3938.
- [16] J. J. P. Stewart, Optimization of parameters for semiempirical methods V: Modification of NDDO approximations and application to 70 elements, *J. Mol. Model.*, Vol. 13, 2007, pp. 1173-1213.
- [17] M. Predota, M.L.Machesky, D.J. Wesolowski, P.T. Cummings, Hydrogen Bonding at the Rutile (110) Surface - Aqueous Interface. *CIMTEC Proceedings*, 2004, pp. 581-588.
- [18] S. Pivovarov, Structure of the oxide-solution interface, *Encyclopedia of Surface and Colloid Science*, Marcel Dekker, Inc., 2002, pp.1-9.
- [19] HyperChem 5.11 Pro, HyperCube Inc., U.S.A., <http://www.hyper.com>

- [20] R. W. G. Wyckoff, *Crystal Structures*, Vol. 1, Second edition, Interscience Publishers, New York, 1963.
- [21] Winmostar v.3.59c, Winmostar by Delphi, Norio Senda.
- [22] A. Pedretti, L. Villa, G. Vistoli, VEGA: A versatile program to convert, handle and visualize molecular structure on windows-based PCs, *J. Mol. Graph.*, Vol. 21, 2002, pp. 47- 49.
- [23] P.W. Atkins, *Physical Chemistry*, Fifth Edition, Oxford University Press, Oxford-Melbourne-Tokyo, 1994, Romanian Translation, Editura Tehnica, Bucuresti, 1996, pp. 614
- [24] C.D. Nenitescu, *Chimie Generala*, Ed. Didactica si Pedagogica, Bucuresti, 1972, pp. 235, pp. 525
- [25] T. Nagao, *Hakodate Kogyo Koto Senmon Gakko Kiyo*, Vol. 27, 1993, pp. 111 -120.